

LEXI: Lossless Exponent Coding for Efficient Inter-Chiplet Communication in Hybrid LLMs

Miao Sun, Alish Kanani, Kaushik Shroff, and Umit Ogras

Department of Electrical and Computer Engineering, University of Wisconsin-Madison
 {smiao23,ahkanani,kshroff,uogras}@wisc.edu

Abstract

Data movement overheads increase the inference latency of state-of-the-art large language models (LLMs). These models commonly use bfloat16 (BF16) format for stable training. Floating-point standards allocate eight bits to the exponent, but our profiling reveals that exponent streams exhibit fewer than 3 bits Shannon entropy, indicating high inherent compressibility. To exploit this potential, we propose LEXI, a novel *lossless exponent compression scheme* based on Huffman coding. LEXI compresses activations and caches on the fly while storing compressed weights for just-in-time decompression near compute, without sacrificing system throughput and model accuracy. The codecs at the ingress and egress ports of network-on-chip routers sustain the maximum link bandwidth via multi-lane LUT decoders, incurring only 0.09% area and energy overheads with GF 22 nm technology. LEXI reduces inter-chiplet communication and end-to-end inference latencies by 33–45% and 30–35% on modern Jamba [23], Zamba [11], and Qwen [3] LLMs implemented on a homogeneous chiplet architecture.

1 Introduction

Increasing demand for LLM-based generative pre-trained transformer (GPT)-class services pressures compute and storage resources. For example, Llama [39], Falcon [2], and Qwen [3] models have scaled to hundreds of billions of parameters, while their computational loads have grown from approximately 100 TeraFLOPS to 1 PetaFLOP per inference. The inference latency is increasingly dominated by data movement as (i) the sheer size of model parameters stresses memory capacity and bandwidth, and (ii) the key-value (KV) cache inherent to self-attention grows with sequence length [8, 21]. These challenges are amplified in multi-die/chiplet accelerators, where cross-die traffic during the decode phase becomes a first-order bottleneck [35]. Quantization and pruning can remedy these problems, but they sacrifice model accuracy for efficiency [14, 38].

Hybrid models that integrate Transformer and Mamba modules have recently emerged as promising solutions toward balancing memory footprint, computational intensity, performance, and accuracy [6, 11, 23]. These architectures reduce KV cache pressure by substituting some attention blocks with fixed-size (sequence-length independent) state-space layers [13]. Despite these improvements, inter-die communication overheads remain a first-order bottleneck [41]. Hence, this paper targets the data transfer overhead, a critical issue because LLM execution is fundamentally limited by memory bandwidth in data-intensive phases [27, 37].

The BF16 format has become the dominant precision for neural network training and inference, particularly in GPU- and cloud-computing environments. For example, the Hugging Face Model Hub, an industry standard platform, declared BF16 as the default precision for most widely adopted LLMs. Indeed, the configuration

metadata of prominent LLMs, such as the Llama and Mistral series, specify the `torch_dtype` as `"bfloat16"`. Using 8-bit exponents, BF16 achieves the same dynamic range as FP32, mitigating overflow and underflow without the explicit loss scaling often required by FP16. However, our profiling shows that the exponent field exhibits on average fewer than 3 bits Shannon entropy during inference due to the limited span of the weights and runtime activations. *This phenomenon offers an opportunity to reduce communication costs without altering numerical accuracy.*

To exploit this potential, we propose LEXI, a lossless exponent coding for efficient inter-chiplet communication. LEXI compresses exponents while preserving the numerical representation of BF16 in memory and compute units, as illustrated in Figure 1. It transfers the weights and activations in a compact lossless form, thereby reducing data-movement latency across memory hierarchies and chiplet interconnects. The design has two paths: (i) offline compression of weights stored in DRAM/high-bandwidth memory (HBM), and (ii) on-the-fly compression of activations, KV caches in attention blocks and state caches in SSM blocks, collectively referred to as *hybrid caches*. A novel lightweight multi-cache Huffman encoder maintains exponent frequency statistics, generates per-layer codebooks, and compresses exponent streams at runtime, with a small codebook piggybacked alongside the bitstream. On the receiving side, a multi-stage lookup table-based decompression provides a single-cycle decode, maintaining pipeline throughput.

We implemented LEXI using GlobalFoundries (GF) 22 nm technology and integrated it on a representative homogeneous multi-chiplet architecture [34]. Since LEXI affects only inter-chiplet and memory-chiplet communication, it is orthogonal to the computations within the chiplet. In our setup, we simulate communication traffic generated by three recent and representative LLMs: Jamba-tiny-dev [23], Zamba2-1.2B-Instruct-v2 [11], and Qwen1.5-1.8B-Chat [3] across WikiText-2 [26] and Colossal Clean Crawled Corpus (C4) [31] datasets. LEXI reduces communication latency by 33–45% and end-to-end inference latency by 30–35%, all while maintaining lossless operation. Our GF 22 nm implementation shows only 0.09% area overhead for these runtime compression /decompression units, highlighting LEXI’s practicality.

To our knowledge, this work is the first to show that exponent-only lossless coding can be implemented at full speed with negligible area and energy overhead. Our major contributions are:

- A novel exponent-only compression scheme for BF16 format, which targets the weights, activations, and hybrid caches in state-of-the-art LLMs.
- Efficient hardware implementation of exponent-only codecs and their seamless integration at the NoC routers and I/O with negligible area overhead using GF 22 nm technology.

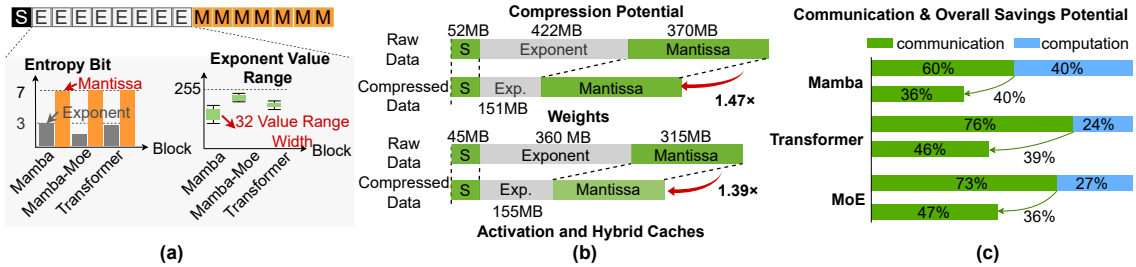


Figure 1: Exponent compression opportunities on NVIDIA GeForce RTX 3090 [29]. (a) BF16 exponents show only ~3 bits of Shannon entropy and span fewer than 32 values, while mantissas consistently use the full 7-bit range. (b) Exponent compression shrinks weights from 422 MB to 151 MB and activations/caches from 360 MB to 155 MB. (c) Lossless exponent compression reduces communication overhead by 36-40% across Mamba, Transformer, and MoE blocks.

- Comprehensive performance evaluations on a multi-chiplet platform, demonstrating significant performance gains and up to 35% lower end-to-end inference latency.

2 Related Work

The growing scale of LLMs has shifted inference bottlenecks from compute to data movement, especially during decode phase [1, 33]. Generating a single token in this phase requires accessing all model weights and hybrid caches from the prior context, creating a disparity between processor speed and available memory bandwidth, commonly referred to as the “memory wall” [10, 28]. This phenomenon reflects the low compute intensity of LLM workloads, where the ratio of FLOPs to bytes transferred is insufficient to hide memory latency, resulting in the under-utilization of compute resources.

Hybrid LLM models complement Transformer attention layers with Mamba SSM layers with fixed-size recurrent state, alleviating memory requirements [9, 13]. For example, Jamba [23] and Zamba [11] achieve 3× and 1.6× faster inference than Mixtral [18]. On edge computing platforms, as demonstrated by eMamba [20], which achieves 2.22× and 9.95× higher throughput compared with Transformer and CNN, respectively. However, algorithmic improvements alone are insufficient to minimize the communication overheads since hybrid models remain memory-bound during inference due to fundamentally autoregressive decode phases. Quantization of weight and activations all the way to extreme two bits [25, 42] and pruning [16] have commonly been used to reduce model size, area and communication overhead. However these approaches sacrifice the model performance. In contrast, LEXI addresses this gap through a hardware-implemented, lossless compression scheme that targets exclusively the exponent field of BF16 data. As an orthogonal approach, LEXI can be seamlessly combined with existing quantization and pruning techniques. Hence, it can be applied after any quantization or pruning technique to further reduce the communication overhead *without impacting the model performance*.

Table 1: Methodology comparison against related work.

Work	Lossless	Compressed Data	Implementation
HACK [45]	✗	KV-cache	SW
KVComp [19]	✗	KV-cache	SW
Ecco [7]	✗	KV-Cache/Act./Weight	HW
Zhang et. al [44]	✓	Weight	SW
Huff-llm [43]	✓	Weight	SW
Zipnn [15]	✓	Weight	SW
LEXI	✓	KV-Cache/Act./State/Weight	HW

Data compression has been effective in reducing on-chip network traffic [32, 40]. Several lossy and lossless compression techniques have been proposed to reduce the storage and communication costs of deep learning models. As shown in Table 1, prior work has largely focused on lossy compression [7, 19, 45], which degrades the performance of the original models. Moreover, existing work on lossless compression [15, 43, 44] has only considered weight compression (e.g., for loading model parameters from the HBM) without addressing the cross-die communication cost. Furthermore, software (SW) compression schemes do not address the dataflow and interconnect bottlenecks of chiplet-based accelerators, where inter-chiplet communication remains a primary constraint. Thus, the focus shifts to dedicated hardware (HW) solutions.

In contrast to prior work, LEXI applies *lossless compression to weights, activations, and hybrid caches*. We present a low-cost hardware implementation to the communication latency while avoiding compute overhead. Our novel design requires a small alphabet and lookup tables (LUTs) with only 0.09% area overhead while achieving full speed (one exponent/cycle) without any performance loss.

3 Exponent Statistics Profiling and Motivation

We first analyze the bit-level entropy in weights, activations, and hybrid caches to analyze potential savings and guide the design process. This profiling exposes redundancies in BF16 representation during inference and highlights the key challenges for practical, hardware-efficient compression.

3.1 Profiling Methodology and Illustrative Results

We run the target workloads on a workstation with an NVIDIA GeForce RTX 3090 GPU [29]. Our instrumented inference script logs (i) weights, (ii) activations, and (iii) hybrid caches (i.e., the Transformer KV cache and the Mamba state cache) at layer boundaries. At execution, each BF16 value is parsed into its {sign, exponent, mantissa} fields and computes the entropy for the exponent stream.

Profiling the Jamba-tiny-dev model over a 1K-token WikiText-2 sequence (Fig. 1) shows that the BF16 exponent stream exhibits at most ~3 bits of entropy, indicating substantial lossless compressibility. This stems from their narrow dynamic range, with most exponent values *concentrated within 32 distinct values*. In contrast, the mantissa consistently uses its full 7-bit precision and offers little compression potential.

Leveraging this property, as shown in Fig. 1(b), LEXI can reduce the exponent volume from 422 to 151 MB for weights and 360 to 155

MB for activations and hybrid caches, corresponding to overall data-volume reductions of 1.47× and 1.39×, respectively. As presented in Fig. 1(c), these savings translate directly into communication cost reduction by 40%, 39% and 36% in Mamba, Transformer, and mixture-of-experts (MoE) blocks, respectively.

3.2 Motivation and Design Challenges

The profiling results indicate that exploiting the redundancy in BF16 exponents can substantially decrease the communication overhead. Realizing this potential during inference requires tackling two primary challenges.

Challenge 1 - Real-time data compression: Compression and decompression must sustain link-rate throughput with a short deterministic latency so that their overheads do not outweigh the reduced transfer time. This requires a streaming operation with (1) flit-aligned framing, (2) fast dynamic codebook configuration, and (3) decoder latency compatible with ingress timing. This demands transforming complex Variable-Length Coding into a predictable cycle-count hardware pipeline. The compression scheme employs a dedicated circuit with minimal internal dependencies to ensure true link-rate throughput, mitigating the scheduling challenges caused by variable output size.

Challenge 2 - Hardware overhead: The compression and decompression units must incur minimal area overhead, avoiding wide datapath overheads and large buffer costs for a chiplet-ready design. Conventional entropy coders are impractical due to sizable dictionaries/SRAMs, deep FIFOs, and long critical paths [22, 24], which inflate area and dynamic power. A chiplet-ready design must avoid wide datapath overheads and meet frequency targets without large buffer costs. This requires minimal-state, context-aware encoding optimized for BF16 exponent content, favoring minimal-sized dictionaries. Achieving high clock speed relies on shallow, heavily pipelined logic to maintain a short critical path, structuring the final hardware to rely primarily on combinational logic rather than large storage structures.

The proposed LEXI framework is designed to solve these challenges. Its streaming, exponent-aware, and hardware-efficient design exploits bit-level redundancy without altering BF16 semantics.

4 LEXI: Entropy-Aware Exponent Compression

4.1 Definitions and LEXI Architecture Overview

Interfacing with Processing Elements (PEs) within chiplets:

The proposed LEXI framework is oblivious to the computations within each PE. The compression and decompression circuits reside on the interconnection network egress and ingress paths as shown in Figure 2. **Activations and hybrid caches** are produced at runtime at compute chiplets in standard (decompressed) format. To minimize the transfer time to their destinations, the exponent components are compressed on-the-fly at egress, before transmission. Then, the receiving unit (compute chiplet) decompresses them before using. In contrast, **the model weights** are assumed to be compressed offline and stored in compressed format in memory to reduce their footprint. When requested, the memory unit transmits them in this format. The receiving compute chiplet decompresses them at ingress on-the-fly before using.

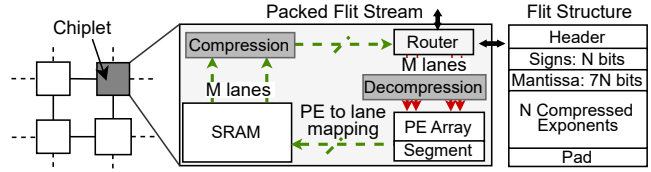


Figure 2: Overview for proposed compression/decompression units in chiplet system.

Huffman tree generation boundary: Generating a new Huffman tree for each layer’s output increases locality (hence, compression ratio) as opposed to using a single tree across the entire inference execution. Once a PE array in a chiplet finishes computations, it produces a fixed number of activations per layer (e.g., 2M activations on average for Qwen1.5-1.8B-Chat model with 1K input tokens when it is mapped to our representative homogeneous chiplet architecture [34] in our experimental evaluations). We initiate tree generation with the first 512 activations, incurring the 78 – cycle penalty only once. The subsequent ~1.9M of activations leverage this tree with zero overhead. Empirical results show that the exponent distribution remains stable across a layer’s outputs because repeated layer-normalization operations keep the activations within a bounded and consistent range. In this way, the proposed LEXI framework (1) benefits from a custom Huffman tree for each set of layer outputs, and (2) incurs a small one-time cost while leveraging the same tree for all remaining activations.

Flow control unit (flit): On-chip and inter-chiplet networks transmit packetized data in packets in units called flits (one flit is sent per cycle). To sustain this maximum link bandwidth, LEXI puts the compressed activations into flits with the following format:

{Header, Sign bits, Mantissa, Compressed Exponents}

The Header indicates how many activations are sent in a given flit, as shown in Figure 2. If the exponent stream does not end on a flit boundary, the remainder is zero-padded. Our design enables streaming flit-aligned transfers without intermediate expansion. At the ingress, the decoder reads the header and reassembles the decompressed activations before passing them back to the PEs.

4.2 Runtime Huffman Tree Generation

LEXI generates a Huffman tree in two steps: 1) constructing a global histogram of exponent frequencies, and 2) codebook generation.

4.2.1 Parallel Histogram Generation: LEXI compresses the activations on-the-fly at the egress boundaries as PEs send them to the interconnection network, as discussed in Section 4.1. To prevent throughput bottlenecks, as shown in Figure 3, it distributes the exponent counting process for histogram generation across M parallel lanes, each equipped with its own local cache. The optimal value of M is found through design space exploration (Section 5.2).

Operations at each lane: As the exponents arrive from the PE array, the first step is checking whether they are already in the local cache with a current count. If the newly arrived exponent is already in the local cache (a cache hit), the lane simply increments its local counter. Our novel M -lane design ensures high locality and hit rate at each lane-specific local cache. In case of a cache miss, the oldest exponent is evicted from the local cache and written to the global histogram with its accumulated count. Then, the new

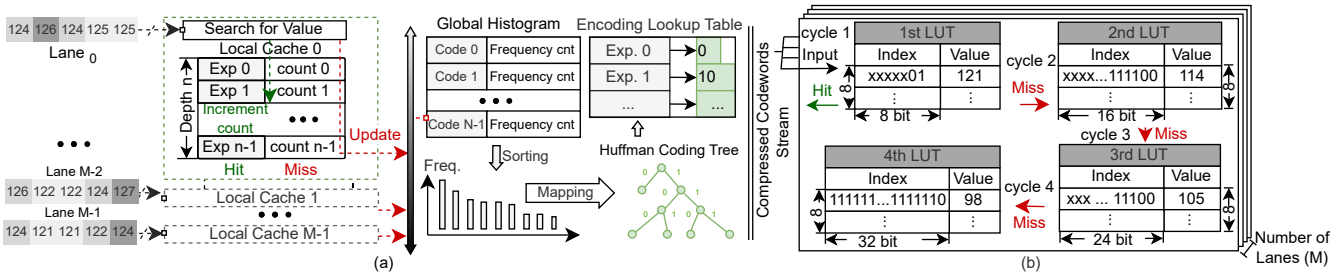


Figure 3: Hardware microarchitecture of LEXI: (a) compression circuit with M parallel lanes, where per-lane local caches accelerate Huffman tree creation and a simple lookup table encodes exponents; (b) Four-stage decompression unit, each stage containing eight entries indexed by 8-, 16-, 24- and 32-bit indices.

entry is written to the cache with a count of one. Our design space exploration in Section 5.2 shows that a cache of eight entries per lane optimizes the balance hit rate and area cost.

Global histogram updates: The global histogram accumulates exponent counts from parallel write operations by the local caches. Competition for histogram port access is resolved via a simple arbiter. The arbiter grants exclusive use to the first arriving request for a fixed duration of three cycles before release. The merged global histogram is then read by the Huffman tree builder to emit the codebook.

4.2.2 Pipelined Codebook Generation Hardware. After receiving all activations required for the Huffman tree generation, the global histogram contains the frequency counts for all observed exponents. Profiling results show consistently fewer than 32 distinct exponent values. Hence, the primary pipeline is designed for this 32-entry range; exceptional values are managed via a fallback mechanism (as detailed at the end of this section). With this data, the tree generation proceeds in three pipelined stages:

1. Sorting the exponents in descending order of their counts: We employ a parallel bitonic sorter [4] optimized for small input sizes (≤ 32 elements). The sorter requires $\log_2(32) \times (\log_2(32) + 1)/2 = 15$ stages, completing in 15 cycles. This balances area efficiency with throughput requirements.

2. Huffman coding tree construction: Following canonical Huffman procedures [17], we build the code tree by repeatedly merging the two least-frequent symbols. Our hardware implementation uses a priority queue backed by the sorted frequency list, requiring 31 cycles for worst-case tree construction (32 elements).

3. Code assignment and LUT programming: The tree is traversed to generate prefix-free codes, with code lengths stored in the encoding LUTs across all M lanes. This requires 32 cycles to program all LUT entries. The entire process completes in 78 cycles (15+31+32), which is seamlessly pipelined with the incoming data stream for on-the-fly compression.

Exception handling for guaranteed functional correctness: To ensure correctness against raw exponents exceeding the 32-entry encoding limit, a lookup miss triggers a 32-bit fallback: a reserved 24-bit escape code (all ones) followed by the raw 8-bit exponent. Since such exceptions are extremely rare (not observed in our experiments), this mechanism imposes negligible bandwidth overhead while maintaining functional integrity.

4.3 Parallel Stream Encoding and Transmission

Following the pipelined codebook generation, LEXI immediately commences continuous, high-throughput encoding.

Distributed parallel lookup: To eliminate lookup contention and maximize throughput, LEXI replicates the 32-entry encoding LUT constructed during codebook generation at each parallel lane. This ensures all M lanes perform simultaneous, single-cycle lookups, transforming the 8-bit exponent into its codeword.

Flit-aligned packetization: A critical step for sustaining the maximum throughput is aggregating the variable-length codewords efficiently. The network interface receives the stream of codewords from all lanes, along with their associated sign and mantissa bits, and packs them into fixed-size flits. Since Huffman codes are **prefix-free**, a minimal, per-layer codebook header is simply prepended to the compressed stream for lossless decoder reconstruction.

Sustained line rate operation: *The entire data path forms a non-blocking pipeline, sustaining one-flit-per-cycle output rate for full inter-layer link bandwidth utilization.* Although an initial startup latency of 78 cycles (78 ns under 1 GHz in our experiments) is incurred once per layer, this cost is negligible against millisecond-scale communication of millions of activations. Crucially, the effective overhead vanishes and maximum link utilization is maintained because all encoding steps (histogram accumulation, tree creation, LUT programming) are fully pipelined with subsequent data.

4.4 On-the-fly Decompression Circuit

Since Huffman decoders process a variable-length bitstream, finding codeword boundaries is inherently sequential. A naive implementation uses a single large LUT indexed by L_{max} (24 bits) to return {exponent, bit-length} in one cycle, but incurs prohibitive area cost and poor scalability. Thus, we design a multi-stage decompression circuit (Figure 3(b)). This multi-stage LUT segments the codebook based on frequency and code length. Stage 1 indexes the first B_1 bits; it returns the symbol if available, else redirects to the next stage. Each subsequent stage k then consumes the additional B_k bits and repeats until the symbol is resolved. Since shorter, high-frequency codes are often resolved in Stage 1 (one cycle), only longer, rarer codes traverse deeper stages.

The key design choice lies in determining the optimal bit-width for each stage. Through extensive design space exploration across all target workloads, we found that a four-stage configuration with $B_1, B_2, B_3, B_4 = 8, 16, 24, 32$ bits provides the optimal balance between area efficiency and decoding latency, as detailed in Section 5.2.

The final stage can also program the reserved escape code. To sustain required throughput, we instantiate multiple parallel decode lanes, distributing incoming flits in a round-robin manner for independent, parallel decoding. This configuration proved area-efficient and line-rate capable, as analyzed in Section 5.2.

5 Implementation and Evaluation of LEXI

5.1 Experimental Setup

Models and datasets: The proposed compression technique is evaluated using two hybrid models Jamba-tiny-dev (319M) [23], Zamba2-1.2B-Instruct-v2 [11]) and one transformer-only model (Qwen1.5-1.8B-Chat [3]). In the remainder of this section, we refer to these models as Jamba, Zamba, and Qwen for simplicity. All three models are tested using WikiText-2 [26] and C4 [31] datasets, with input sequence lengths of 1K and 2K tokens, respectively. In both cases, the output sequence length is fixed at 512 tokens.

Target hardware: To demonstrate LEXI, we integrated it into a 6x6 homogeneous chiplet array based on the Simba [34] architecture. This test case is selected since it was validated with hardware implementation. It uses a 2D mesh network-on-interposer (NoI) with 100 Gbps inter-chiplet links. Each chiplet executes block-level kernels (Mamba/SSM, attention, and feed-forward). LEXI transmits compressed weights and decompresses the weights on-the-fly before use. Hybrid caches are compressed block-by-block when written back to memory, then retrieved and decompressed just prior to computation. Activations are transmitted between chiplets in compressed form and decompressed before being used. Inter-chiplet transfers are modeled using a modified cycle-accurate HeteroGarnet simulator [5], extended to support trace-driven traffic.

Hardware implementation: We implemented the proposed compression/decompression units using SystemVerilog. It is synthesized at a target operating frequency of 1 GHz using the Synopsis Design Compiler with the GF 22 nm technology node.

5.2 Area-Performance Trade-off Optimization

Compressor trade-offs: The compressor consists of multi-lane caches, which have two knobs: per-lane cache depth and the number of lanes. Figure 4 plots the local cache hit rate versus its depth during the encoding phase. A depth of 8 entries per lane achieves over 90% average hit rate for all tested models. Given the diminishing returns of larger sizes, we adopt 8-entry caches in each lane. Next, we analyze the total cache size to optimize codebook creation latency. Figure 5 shows this trade-off for the codebook generation latency with 512 activations. While a single lane with depth 4 is area-efficient, it requires 788 ns to complete at 1 GHz. At the other

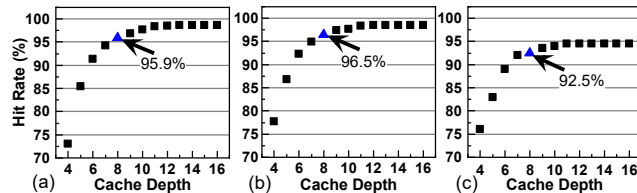


Figure 4: Local cache hit rate vs. cache depth on WikiText-2 for three models: (a) Jamba, (b) Zamba, (c) Qwen

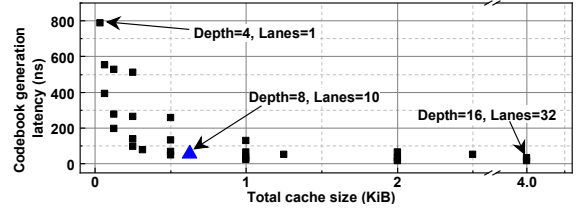


Figure 5: Codebook generation latency vs. cache size with 512 activations in BF16.

extreme, 32 lanes with depth 16 reduce the latency to 17 ns, but the total cache size grows to 4 KiB. We select a balanced design point with 10 lanes and depth 8, which achieves codebook creation in about 55 ns with only 0.625 KiB of cache.

Decompressor tradeoffs: To analyze the latency–area trade-offs in the decompression unit, we implemented it using different multi-stage LUTs configurations. As shown in Figure 6, a 4-stage LUT decoder indexed by 8/16/24/32-bit prefixes achieves an average latency of 11.6 ns with an area of 98.5 μm^2 . For comparison, a single 32-bit LUT table achieves a slightly lower latency of 10 ns but requires 157.6 μm^2 area, making it less area-efficient. The most optimistic case, required to saturate the 100 Gbps link, involves 10 compressed values (each 10 bits: 2-bit codeword + 1-bit sign + 7-bit mantissa). Thus, ten decode lanes we searched based on Figure 5 are sufficient to sustain the full link bandwidth, distributing incoming flits in a round-robin manner. This design balances throughput and cost, delivering near line-rate performance with modest overhead.

5.3 Communication and End-to-End Execution Time Evaluation

This section evaluates the BF16 exponent compression ratio (CR) for the Jamba, Zamba, and Qwen models. As shown in Table 2, LEXI yields the highest CR $\approx 3.1\times$, by leveraging per-layer frequency distribution. This significantly surpasses base-delta-immediate (BDI) compression [30] (2.40 \times), which utilizes micro-local value correlation via 3-bit delta encoding. Conversely, the CR of run-length encoding (RLE) [12] $\approx 0.64\times$, results in data expansion, confirming that long runs of identical exponent values are infrequent. The primary compression potential thus lies in repeated value frequency, which Huffman coding leverages.

Next, we analyze the impact of LEXI on communication latency and overall execution time. Table 3 reports communication time for uncompressed, weight-only, and LEXI (offline weights + on-the-fly activations/caches). On WikiText-2, uncompressed latency for Jamba is 86.70ms. LEXI reduces this latency by 45.4% to 47.35ms,

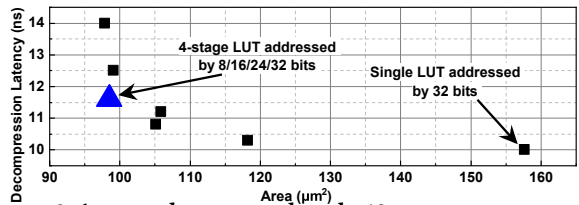


Figure 6: Average latency to decode 10 exponents versus decoder area. The highlighted point marks our chosen 4-stage LUT decoder with tables addressed by 8/16/24/32-bit prefixes, eight entries per stage.

Table 2: Compression Ratio Comparison among different compression methods on different LLM weights

Model/Layer	Base	RLE [12]	BDI [30]	LEXI
Jamba-mini	1.00×	0.62×	2.43×	3.14×
Zamba2-1.2B	1.00×	0.65×	2.36×	3.07×
Qwen1.5-1.8B	1.00×	0.64×	2.40×	3.12×

Table 3: Communication latency (ms) of Jamba, Zamba, and Qwen models on WikiText-2 and C4 datasets.

Datasets	Methods	Jamba	Zamba	Qwen
WikiText-2	Uncompressed	86.70	8539.52	1644.07
	Compressed weights	80.62	8522.16	1631.17
	LEXI	47.35	5682.26	1014.30
C4	Uncompressed	294.86	12315.53	2814.40
	Compressed weights	283.45	12262.64	2788.61
	LEXI	171.03	8128.71	1711.34

achieving 33.5% and 38.3% reduction for Zamba and Qwen, respectively. On the C4 dataset, LEXI similarly decreases communication by 42.0% for Jamba, 34.0% for Zamba, and 39.2% for Qwen. These results underscore the effectiveness of dynamic Huffman compression during LLM inference.

Finally, we evaluate the end-to-end execution time on the Simba architecture [34]. Since compression does not alter the arithmetic operations, computation latency remains identical in uncompressed and compressed settings. Across both datasets, communication latency accounts for 68–95% of the end-to-end latency in the uncompressed case. Figure 7 shows that LEXI substantially reduces this bottleneck, delivering 30–35% reductions in end-to-end inference time across model types and datasets. Specifically, it lowers the end-to-end latency on the WikiText-2 dataset by 31%, 32%, and 30% for Jamba, Zamba, and Qwen, respectively. Similarly, the end-to-end latency is reduced by 35%, 32%, and 31% on the C4 dataset.

5.4 Hardware Overhead and Power Analysis

This section evaluates the area and power consumption overheads. Table 4 reports post-synthesis results in GF 22 nm for the configuration selected in Section 5.2. The compressor employs 10 parallel lanes, each with an 8-entry local frequency cache, alongside a

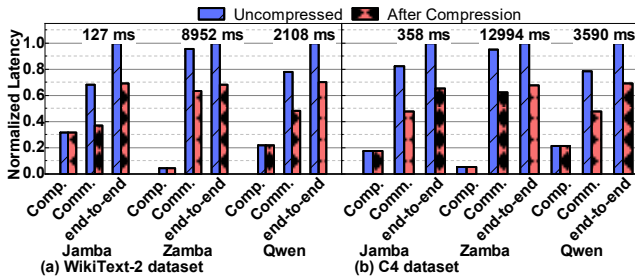


Figure 7: Normalized average end-to-end latency for Jamba, Zamba, and Qwen models on (a) WikiText-2 with 1K input tokens and (b) C4 with 2K input tokens, each generating 512 output tokens. Annotated numbers indicate the uncompressed end-to-end latency.

Table 4: Area and power breakdown of compression and decompression units in GF 22 nm tech node.

Metric	Comp. Units			Dec. Unit
	Local Cache	Global Hist. & Code Gen.	Enc. LUT	Dec. LUT
Area (μm^2)	9.85	13113	79.87	98.5
Power (mW)	0.25	5.23	1.74	2.03
Lanes	$\times 10$	$\times 1$	$\times 10$	$\times 10$
Total Area (μm^2)	98.5	13113	798.7	985
Total Power (mW)	2.5	5.23	17.4	20.3

shared global histogram for tree construction. The encoding stage uses 10 parallel LUTs. The decompressor is a multi-stage LUT design with four stages, each containing 8 entries and indexed by 8/16/24/32-bit prefixes.

Compressor: The compression unit includes: (1) 10 local caches ($9.85 \mu\text{m}^2$ each with 2.5 mW total power consumption), (2) a single global histogram and codebook generation circuit ($13,113 \mu\text{m}^2$, 5.23 mW), and (3) 10 encoding LUTs (each $79.87 \mu\text{m}^2$, with 17.4 mW total power consumption).

Decompressor: Multi-stage decoding LUTs occupy $98.5 \mu\text{m}^2$ area each, for a total $985 \mu\text{m}^2$ area and 20.3 mW power consumption.

Overall area and comparisons: All the circuits within LEXI occupy $14,995.2 \mu\text{m}^2$ and consume 45.43 mW total power. For a fair comparison with the 16 nm Simba system, we scale our results using [36], resulting in a total LEXI area of $5,452.8 \mu\text{m}^2$. Given that each Simba chiplet has 6 mm^2 area, the LEXI overhead corresponds to just 0.09% of chiplet area, demonstrating that the compression/decompression logic introduces negligible hardware overhead.

6 Conclusions

This paper presented LEXI, a lightweight, entropy-aware exponent compression framework designed to accelerate LLM inference on chiplet-based systems. Bit-level profiling of weights, activations, and hybrid caches shows that exponents require fewer than three bits, on average, revealing substantial compression opportunities. To enable real-time operation, we designed a Huffman-based encoding/decoding framework with parallel multi-lane local caches for tree construction and efficient encoder–decoder LUTs. The proposed design generates codebooks and compressed flits at line-rate (i.e., without impacting throughput). Integrated into the Simba chiplet architecture, LEXI reduces inter-chiplet communication latency by 33–45% and improves end-to-end inference time by 30–35% across Jamba, Zamba, and Qwen models on WikiText-2 and C4 datasets. Hardware synthesis in GF 22 nm shows that the design incurs only 0.09% area overhead. Overall, we showed that lossless compression of BF16 exponents is effective and provides a practical and scalable solution to mitigate the memory wall toward more efficient hybrid LLM inference.

Disclosure: Dr. Ogras serves as a contractor for Samsung Austin Research & Development Center and Advanced Computing Lab (SARC/ACL). This relationship has been approved under applicable outside activities policies.

References

- [1] Salma Afifi, Febin Sunny, Mahdi Nikdast, and Sudeep Pasricha. 2024. Accelerating neural networks for large language models and graph processing with silicon photonics. In *2024 Design, Automation & Test in Europe Conference & Exhibition (DATE)*. 1–6.
- [2] Ebtesam Almazrouei, Hamza Alobeidli, Abdulaziz Alshamsi, Alessandro Cappelli, Ruxandra Cojocaru, M erouane Debbah,  tienne Goffinet, Daniel Hesse, Julien Launay, Quentin Malartic, et al. 2023. The falcon series of open language models. *arXiv preprint arXiv:2311.16867* (2023).
- [3] Jinze Bai, Shuai Bai, Yunfei Chu, Zeyu Cui, Kai Dang, Xiaodong Deng, Yang Fan, Wenbin Ge, Yu Han, Fei Huang, et al. 2023. Qwen technical report. *arXiv preprint arXiv:2309.16609* (2023).
- [4] Kenneth E Batchler. 1968. Sorting networks and their applications. In *Proceedings of the April 30–May 2, 1968, spring joint computer conference*. 307–314.
- [5] Srikanth Bharadwaj, Jieming Yin, Bradford Beckmann, and Tushar Krishna. 2020. Kite: A family of heterogeneous interposer topologies enabled via accurate interconnect modeling. In *2020 57th ACM/IEEE Design Automation Conference (DAC)*. IEEE, 1–6.
- [6] Aaron Blakeman et al. 2025. Nemotron-h: A family of accurate and efficient hybrid mamba-transformer models. *arXiv preprint arXiv:2504.03624* (2025).
- [7] Feng Cheng, Cong Guo, Chiyue Wei, Junyao Zhang, Changchun Zhou, Edward Hanson, Jiaqi Zhang, Xiaoxiao Liu, Hai Li, and Yiran Chen. 2025. Ecco: Improving Memory Bandwidth and Capacity for LLMs via Entropy-Aware Cache Compression. In *Proceedings of the 52nd Annual International Symposium on Computer Architecture*. 793–807.
- [8] Tri Dao, Dan Fu, Stefano Ermon, Atri Rudra, and Christopher R . 2022. Flashattention: Fast and memory-efficient exact attention with io-awareness. *Advances in neural information processing systems* 35 (2022), 16344–16359.
- [9] Tri Dao and Albert Gu. 2024. Transformers are ssm: Generalized models and efficient algorithms through structured state space duality. *arXiv preprint arXiv:2405.21060* (2024).
- [10] Amir Gholami, Zhewei Yao, Sehoon Kim, Coleman Hooper, Michael W Mahoney, and Kurt Keutzer. 2024. Ai and memory wall. *IEEE Micro* 44, 3 (2024), 33–39.
- [11] Paolo Glorioso, Quentin Anthony, Yury Tokpanov, James Whittington, Jonathan Pilault, Adam Ibrahim, and Beren Millidge. 2024. Zamba: A compact 7b ssm hybrid model. *arXiv preprint arXiv:2405.16712* (2024).
- [12] Solomon Golomb. 1966. Run-length encodings (corresp.). *IEEE transactions on information theory* 12, 3 (1966), 399–401.
- [13] Albert Gu and Tri Dao. 2024. Mamba: Linear-Time Sequence Modeling with Selective State Spaces. In *First Conference on Language Modeling*.
- [14] Song Han, Huizi Mao, and William J. Dally. 2016. Deep Compression: Compressing Deep Neural Networks with Pruning, Trained Quantization and Huffman Coding. In *International Conference on Learning Representations (ICLR)*. <https://arxiv.org/abs/1510.00149>
- [15] Moshik Hershcovitch, Andrew Wood, Leshem Choshen, Guy Gironmsky, Roy Leibovitz, Or Ozeri, Ilias Ennouri, Michal Malka, Peter Chin, Swaminathan Sundararaman, et al. 2025. Zipnn: Lossless compression for ai models. In *2025 IEEE 18th International Conference on Cloud Computing (CLOUD)*. IEEE, 186–198.
- [16] Yingbing Huang, Lily Jiaxin Wan, Hanchen Ye, Manvi Jha, Jinghua Wang, Yuhong Li, Xiaofan Zhang, and Deming Chen. 2024. New solutions on LLM acceleration, optimization, and application. In *Proceedings of the 61st ACM/IEEE Design Automation Conference*. 1–4.
- [17] David A. Huffman. 1952. A Method for the Construction of Minimum-Redundancy Codes. *Proceedings of the IRE* 40, 9 (1952), 1098–1101. <https://doi.org/10.1109/JRPROC.1952.273898>
- [18] Albert Q Jiang, Alexandre Sablayrolles, Antoine Roux, Arthur Mensch, Blanche Savary, Chris Bamford, Devendra Singh Chaplot, Diego de las Casas, Emma Bou Hanna, Florian Bressand, et al. 2024. Mixtral of experts. *arXiv preprint arXiv:2401.04088* (2024).
- [19] Bo Jiang, Taolue Yang, Youyuan Liu, Chengming Zhang, Xubin He, and Sian Jin. 2025. KVComp: A High-Performance, LLM-Aware, Lossy Compression Framework for KV Cache. *arXiv preprint arXiv:2509.00579* (2025).
- [20] Jiyong Kim, Jaeho Lee, Jiahao Lin, Alish Kanani, Sun Miao, Umit Ogras, and Jaehyun Park. 2025. eMamba: Efficient Acceleration Framework for Mamba Models in Edge Computing. *ACM Transactions on Embedded Computing Systems* (2025).
- [21] Woosuk Kwon, Zhuohan Li, Siyuan Zhuang, Ying Sheng, Lianmin Zheng, Cody Hao Yu, Joseph Gonzalez, Hao Zhang, and Ion Stoica. 2023. Efficient memory management for large language model serving with pagedattention. In *Proceedings of the 29th symposium on operating systems principles*. 611–626.
- [22] Morgan Ledwon, Bruce F Cockburn, and Jie Han. 2019. Design and evaluation of an fpga-based hardware accelerator for deflate data decompression. In *2019 IEEE Canadian Conference of Electrical and Computer Engineering (CCECE)*. IEEE, 1–6.
- [23] Opher Lieber et al. 2024. Jamba: A hybrid transformer-mamba language model. *arXiv preprint arXiv:2403.19887* (2024).
- [24] Hsin-I Liu. 2010. *Architecture and hardware design of lossless compression algorithms for direct-write maskless lithography systems*. Ph.D. Dissertation. UC Berkeley.
- [25] Zechun Liu, Changsheng Zhao, Hanxian Huang, Sijia Chen, Jing Zhang, Jiawei Zhao, Scott Roy, Lisa Jin, Yunyang Xiong, Yangyang Shi, et al. 2025. Paretoq: Scaling laws in extremely low-bit llm quantization. *arXiv preprint arXiv:2502.02631* (2025).
- [26] Stephen Merity, Caiming Xiong, James Bradbury, and Richard Socher. 2016. Pointer Sentinel Mixture Models. [arXiv:1609.07843](https://arxiv.org/abs/1609.07843) [cs.CL] Introduces the WikiText language modeling dataset (WikiText-2, WikiText-103).
- [27] Abhishek Moitra, Arkapravo Ghosh, Shrey Agarwal, Aporva Amarnath, Karthik Swaminathan, and Priyadarshini Panda. 2025. MEADOW: Memory-efficient Dataflow and Data Packing for Low Power Edge LLMs. *arXiv preprint arXiv:2503.11663* (2025).
- [28] Onur Mutlu, Saugata Ghose, Juan G omez-Luna, and Rachata Ausavarungrun. 2022. A modern primer on processing in memory. In *Emerging computing: from devices to systems: looking beyond Moore and Von Neumann*. Springer, 171–243.
- [29] NVIDIA Corporation. 2020. GeForce RTX 3090. <https://www.nvidia.com/en-us/geforce/graphics-cards/30-series/rtx-3090/> Accessed: 2025-09-11.
- [30] Gennady Pekhimenko, Vivek Seshadri, Onur Mutlu, Phillip B Gibbons, Michael A Kozuch, and Todd C Mowry. 2012. Base-delta-immediate compression: Practical data compression for on-chip caches. In *Proceedings of the 21st international conference on Parallel architectures and compilation techniques*. 377–388.
- [31] Colin Raffel, Noam Shazeer, Adam Roberts, Katherine Lee, Sharan Narang, Michael Matena, Yanqi Zhou, Wei Li, and Peter J. Liu. 2020. Exploring the Limits of Transfer Learning with a Unified Text-to-Text Transformer. *Journal of Machine Learning Research* 21, 140 (2020), 1–67.
- [32] Venkata Yaswanth Raparti and Sudeep Pasricha. 2018. DAPPER: Data aware approximate NoC for GPGPU architectures. In *2018 Twelfth IEEE/ACM International Symposium on Networks-on-Chip (NOCS)*. IEEE, 1–8.
- [33] Pol G Recasens, Ferran Agullo, Yue Zhu, Chen Wang, Eun Kyung Lee, Olivier Tardieu, Jordi Torres, and Josep Ll Berral. 2025. Mind the memory gap: Unveiling gpu bottlenecks in large-batch llm inference. *arXiv preprint arXiv:2503.08311* (2025).
- [34] Yakun Sophia Shao et al. 2019. Simba: Scaling deep-learning inference with multi-chip-module-based architecture. In *Proceedings of the 52nd annual IEEE/ACM international symposium on microarchitecture*. 14–27.
- [35] Harsh Sharma, Pratyush Dhingra, Jana Doppa, Umit Ogras, and Partha Pratim Pande. 2025. A heterogeneous chiplet architecture for accelerating end-to-end transformer models. *ACM Transactions on Design Automation of Electronic Systems* 30, 3 (2025), 1–24.
- [36] Aaron Stillmaker and Bevan Baas. 2017. Scaling equations for the accurate prediction of CMOS device performance from 180 nm to 7 nm. *Integration* 58 (2017), 74–81.
- [37] Yutao Sun, Li Dong, Barun Patra, Shuming Ma, Shaohan Huang, Alon Benhaim, Vishrav Chaudhary, Xia Song, and Furu Wei. 2023. A length-extrapolatable transformer. In *Proceedings of the 61st annual meeting of the association for computational linguistics (volume 1: long papers)*. 14590–14604.
- [38] Zhigang Tao, Tae Jun Oh, Gi-Joon Nam, and Scott A. Mahlke. 2019. Energy-Quality Scalable Neural Networks through Dynamic Precision Scaling. In *Design, Automation & Test in Europe Conference (DATE)*. 137–142. <https://doi.org/10.23919/DAT.2019.8714910>
- [39] Hugo Touvron, Louis Martin, Kevin Stone, Peter Albert, Amjad Almahairi, Yasmine Babaei, Nikolay Bashlykov, Soumya Batra, Prajwal Bhargava, Shruiti Bhosale, et al. 2023. Llama 2: Open foundation and fine-tuned chat models. *arXiv preprint arXiv:2307.09288* (2023).
- [40] Ying Wang, Yinhe Han, Jun Zhou, Huawei Li, and Xiaowei Li. 2016. DISCO: A low overhead in-network data compressor for energy-efficient chip multi-processors. In *Proceedings of the 53rd Annual Design Automation Conference*. 1–6.
- [41] Zheng Xu, Dehao Kong, Jiaxin Liu, Jinxi Li, Jingxiang Hou, Xu Dai, Chao Li, Shaojun Wei, Yang Hu, and Shouyi Yin. 2025. WSC-LLM: Efficient LLM Service and Architecture Co-exploration for Hetero-scale Chips. In *Proceedings of the 52nd Annual International Symposium on Computer Architecture*. 1–17.
- [42] Chenhao Xue, Chen Zhang, Xun Jiang, Zhutianya Gao, Yibo Lin, and Guangyu Sun. 2024. Oltron: Algorithm-Hardware Co-design for Outlier-Aware Quantization of LLMs with Inter-/Intra-Layer Adaptation. In *Proceedings of the 61st ACM/IEEE Design Automation Conference*. 1–6.
- [43] Patrick Yubeaton, Tareq Mahmoud, Shehab Naga, Pooria Taheri, Tianhua Xia, Arun George, Yasmeim Khalil, Sai Qian Zhang, Siddharth Joshi, Chinmay Hegde, et al. 2025. Huff-llm: End-to-end lossless compression for efficient llm inference. *arXiv preprint arXiv:2502.00922* (2025).
- [44] Tianyi Zhang, Yang Sui, Shaochen Zhong, Vipin Chaudhary, Xia Hu, and Anshumali Shrivastava. 2025. 70% Size, 100% Accuracy: Lossless LLM Compression for Efficient GPU Inference via Dynamic-Length Float. *arXiv preprint arXiv:2504.11651* (2025).
- [45] Zeyu Zhang, Haiying Shen, Shay Vargaftik, Ran Ben Basat, Michael Mitzenmacher, and Minlan Yu. 2025. HACK: Homomorphic Acceleration via Compression of the Key-Value Cache for Disaggregated LLM Inference. In *Proceedings of the ACM SIGCOMM 2025 Conference*. 1245–1247.